Journal of Solid Mechanics and Materials Engineering

Vol. 4, No. 1, 2010

Mechanism of Electrical Resistance Change of a Thin CFRP Beam after Delamination Cracking*

Akira TODOROKI**, Yusuke SAMEJIMA***, Yoshiyasu HIRANO****, Ryosuke MATSUZAKI***** and Yoshihiro MIZUTANI*****

** Department of Mechanical Sciences & Engineering,
Tokyo Institute of Technology
2-12-1, Ookayama, Meguro, Tokyo 1528552, Japan
E-mail:atodorok@ginza.mes.teich.ac.jp
*** Graduate student of Tokyo Institute of Technology
**** Supersonic transport team, Aviation Program Group, JAXA,
6-13-1, Osawa, Mitaka-city, Tokyo, 1810015, Japan
***** Department of Mechanical Sciences & Engineering,
Tokyo Institute of Technology

Abstract

This paper considers a detailed mechanism of the electrical resistance change observed after delamination cracking of a thin Carbon Fiber Reinforced Polymer (CFRP) laminate. For this laminate, the electrical resistance increases after delamination cracking, although the electrical resistance decreases after delamination cracking of a thick CFRP laminate. One of the proposed reasons for this difference is the residual strain relief caused by the delamination cracking. We report experimental and FEM analyses to investigate the effect of shut-off of the current path caused by delamination cracking, and the effect of piezoresistance caused by residual strain relief after delamination cracking. Residual strain relief was measured experimentally, and the results compared to the FEM results. On the basis of the FEM results the effect of the piezoresistance was estimated. It was found that the effect of the piezoresistance is small compared to the effect of the current shut-off for the thin CFRP laminate.

Key words: Composites, Carbon, Delamination, Piezoresistance, Residual stress

1. Introduction

Carbon Fiber Reinforced Polymer (CFRP) is widely adopted for aerospace structures because of its high specific strength and stiffness. Although CFRP laminates have superior properties compared to those of conventional metallic materials, CFRP laminates can easily have delamination cracks resulting from small impact loads such as from dropped tools. Since the delamination cracks are usually difficult to be detected by visual inspection, the CFRP laminates must have high knockdown factors or require expensive non-destructive inspection tools to confirm the structural integrity.

The electrical resistance change method is a non-destructive and attractive inspection method that has been the subject of numerous experimental investigations [(1)-(10)]. The method uses carbon fibers as sensors and does not require expensive instruments, and can be used for existing structures. Research on the use of the electrical resistance change method has been reported for monitoring applied strain [(11),(12)], matrix cracking [(13),(14)] and delamination monitoring [(15)-(23)].

For the delamination monitoring of the CFRP laminates, multiple copper electrodes

*Received 19 Aug., 2009 (No. 09-0463)
[DOI: 10.1299/jmmp.4.1]

were made on a single surface of the laminated plate, and the electrical resistances between adjacent electrodes were all measured. The relationship between the delamination and the sets of the measured electrical resistance changes was obtained with artificial neural networks or response surfaces. For thin CFRP laminates the electrical resistance increased after delamination creation [16]-[18]. For thick CFRP laminates, however, the electrical resistance decreased after delamination cracking even though a two-probe method was used [22]. In that work the mechanism of the decrease of electrical resistance after delamination cracking was not clarified, but residual strain relief is implicated in the mechanism. Residual strain relief may also affect a thin CFRP laminate.

The present paper deals in detail with the mechanism of the electrical resistance change of a thin CFRP laminate. A delamination crack shuts off the electric current path and increases electrical resistance, and causes residual strain relief in both the fiber direction and the transverse direction. The residual strain relief causes an electrical resistance change that comes from the piezoresistance (electrical resistance change caused by applied strain) of the CFRP laminates. Although a dent deformation is made at the indentation point for a thick CFRP laminate because of the high compression loading at the indentation point, the dent was not observed for the thin CFRP laminate. The shut-off effect and the residual strain relief effect are compared on the basis of experimental results and FEM analyses. The mechanism of the electrical resistance change for the thin CFRP laminates is clarified.

2. Specimen and experimental method

The material used in the present study was unidirectional carbon/epoxy prepreg produced by Mitsubishi Rayon Co. Ltd. The prepreg production number was PYROFIL #380. As a thin CFRP laminate test piece, a simple eight-ply cross-ply laminate with stacking sequence $[0_2/90_2]$s was used to compare the experimental results with the analytical results of FEM. The CFRP laminates were cured at 130°C and 0.6 MPa for 90 min using an autoclave. Beam type specimens 80 mm long and 20 mm wide were made from the CFRP plate as shown in Fig.1. The thickness of the specimens was approximately 2 mm. and the fiber volume fraction, V_f, was 0.53. Two electrodes were mounted on a single surface of the CFRP beam using an electrical copper plating method. The process used to make the electrodes was as follows:

(1) Polish the target CFRP laminate surface with rough sandpaper #240;
(2) Mask all except the target area with vinyl chloride tape;
(3) Remove sizing around carbon fibers, using several drops of concentrated sulfuric acid;
(4) Clean the specimen surface;
(5) Polish the surface with fine (#400) sandpaper;
(6) Use silver paste to make electrical contact;
(7) Perform the first electrical copper plating at low electric current density (0.66 A dm^{-2}) in a solution of copper sulfate for 30 minutes;
(8) Perform a second copper plating at high electric current density (2.0 A dm^{-2}) for 30 minutes;
(9) Clean the specimen;
(10) Dry the specimen;
(11) Bond lead wire by soldering; and
(12) Cover the electrodes with epoxy adhesive.

To measure the residual strain relief after delamination, three bi-axial strain gages were attached to the surface on which the electrodes were mounted, as shown in Fig.1. To make a

delamination crack in the CFRP beam, an interlaminar shear test was used. The test jig is illustrated in Fig.2; the span length was 15 mm. At the indentation point and support points, a GFRP thin plate (thickness=0.5 mm) and Teflon film (thickness=0.5 mm) were inserted to prevent electrical contact between the specimen and the metallic jig. Coordinates x-y-z were defined as shown in Fig.1. The longitudinal direction of the beam was defined as the x-direction, and the thickness direction as the y-direction.

Electrical resistance change was measured using an LCR meter (Type #3522-50) made by Hioki Co. Ltd. A two-probe method was used. Alternating current (1 kHz and 10 mA) was adopted for the measurements, because alternating current gave more stable measurements than direct current for this LCR meter. The CFRP laminates were modeled as simple orthotropic resistances up to 1 MHz. Thus, the CFRP laminate was treated as a simple electrical resistance for the low frequency alternating current.

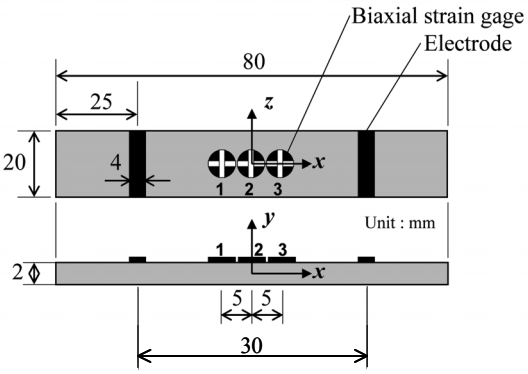

Fig.1 Specimen configuration.

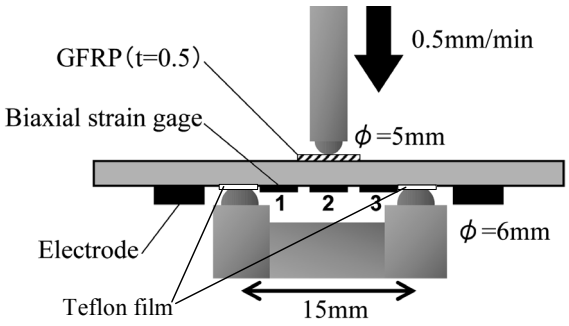

Fig.2 Interlaminar shear test to make a delamination crack.

3. FEM analytical method

To evaluate the effects of shut-off of current path caused by the delamination crack, and piezoresistance caused by strain relief after delamination cracking, three dimensional (3-D) FEM analyses were performed. Figure 3 illustrates the effect of shut-off of the current path. Strong orthotropic conductivity prevents current flow in the 90°-ply, hence there is a current in the thickness direction to make current flow in the bottom 0°-ply. The delamination crack impedes current flow in the thickness direction and increases the electrical resistance by shut-off of the current path.

Figure 4 illustrates the effect of piezoresistance. The delamination crack relieves residual strains caused by the thermal curing process. For example, the transverse direction of the top 0°-ply shrinks and the carbon fiber direction elongates by residual strain relief.

For actual CFRP laminates the electrical contact at the electrodes is not perfect. Consequently longitudinal current flows in the transverse direction as shown in Fig.4. This transverse current implies that the electrical resistance in the fiber direction is affected by the transverse strain, and this effect is not isotropic. Since the residual strain relief is multi-axial strain, the effect of the residual strain relief must be considered as multi-axial loading. Reference (12) shows the experimental work and the piezoresistance of multi-axial loading. Since the material system of that report is the same as the present system, the multi-axial piezoresistance of reference (12) was adopted in the present paper.

$$\begin{Bmatrix} \left(\frac{\Delta R}{R}\right)_L \\ \left(\frac{\Delta R}{R}\right)_T \end{Bmatrix} = \begin{bmatrix} 2.49 & 0.43 \\ -0.42 & 2.38 \end{bmatrix} \begin{Bmatrix} \varepsilon_L \\ \varepsilon_T \end{Bmatrix} \tag{1}$$

where subscripts L and T mean fiber direction and transverse direction, respectively. This effect of the piezoresistance is calculated on the basis of the FEM results.

For the FEM analyses exact conductivity is indispensable. Electric conductivity in the fiber direction (σ_0), transverse direction (σ_{90}) and thickness direction (σ_t) were measured with small sized specimens using the LCR meter. To measure the electric conductivity in the fiber direction a 50 mm long, 20 mm wide small plate specimen was used. The stacking sequence was $[0_8]_T$ for the measurements of conductivity in the fiber direction and in the transverse direction. For the measurements of conductivity in the thickness direction, four types of stacking sequences (two kinds of thickness) were adopted to investigate the effect of the stacking sequences: the four stacking sequences were $[(0/90)_2]$s, $[0_2/90_2]$s, $[(0/90/\pm45)_2]$s and $[(0/90)_4]$s. The thickness of the eight-ply laminates was approximately 2 mm and that of 16-ply laminates was approximately 4 mm.

Using the measured conductivities in the three directions, FEM analyses were performed with the commercially available FEM code ANSYS ver.11. For the 3D-FEM analyses, eight-node solid elements were adopted. At the electrodes, all surface nodes were coupled to have the same voltage, to simulate the copper electrodes. At the left electrode an electric current of 10 mA was applied, and the voltage of the right electrode was kept at zero. From the calculated voltage at the left electrode electrical resistance was calculated. The element dimension was 2 mm (length)×2 mm (width)×0.125 mm (thickness). For the 3-D FEM analyses of the beam type specimen, the total number of nodes was 7854 and the total number of elements was 6560. The mesh division is rough because only the rough estimation of the residual strain is required here.

To investigate the effect of shut-off of current path, a delamination crack with a matrix crack was made in the FEM model. The crack dimension and the location were modeled using the experimental results. The matrix crack, however, is modeled as a straight vertical crack to simplify the FEM mesh division. The delamination crack was simulated as an electric insulator, and doubly defined nodes were separated at the delamination crack line. In the present study, the crack surface contact is not considered to simplify the analyses.

To investigate the effect of residual strain relief (the effect of piezoresistance), thermal deformation analyses of specimens with and without a delamination crack were performed. By subtracting the strain of the specimen with a delamination crack from the strain of the specimen without a delamination crack, residual strain relief was calculated. By averaging the relieved residual strain in the elements between the two electrodes, the electrical resistance change caused by the piezoresistance was roughly estimated.

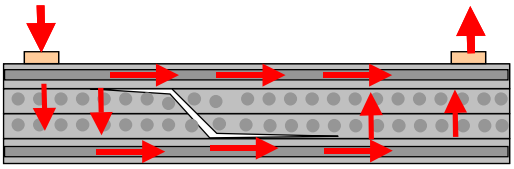

Fig.3 Illustration of shut-off of current path.

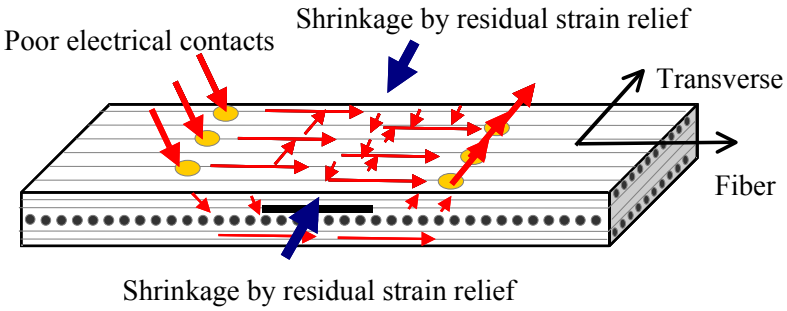

Fig.4 Illustration of piezoresistance effect.

4. Experimental and FEM results

Figure 5 shows load-displacement and electrical resistance–displacement curves measured during loading. The solid curve shows the results of the electrical resistance change, and the broken curve the results of the load. The abscissa is the time. Since the test was performed under the constant displacement rate condition, time is equivalent to the displacement. With increase of the indentation load (compression load) the electrical resistance increased, and the electrical resistance remained positive after delamination creation at complete unloading.

Figure 6 shows the results of the specimen side surface observed after delamination creation. The delamination crack configuration is reversed Z-type with a matrix crack. The delamination length of both interlaminas (upper and lower) is the almost same. The measured strain after the creation of the delamination crack is shown in Fig.7. The ordinate is the measured strain, and the abscissa denotes the strain gage. The first letter is the strain gage number, and the second letter is the strain direction (0 means fiber direction and 90 means transverse direction).

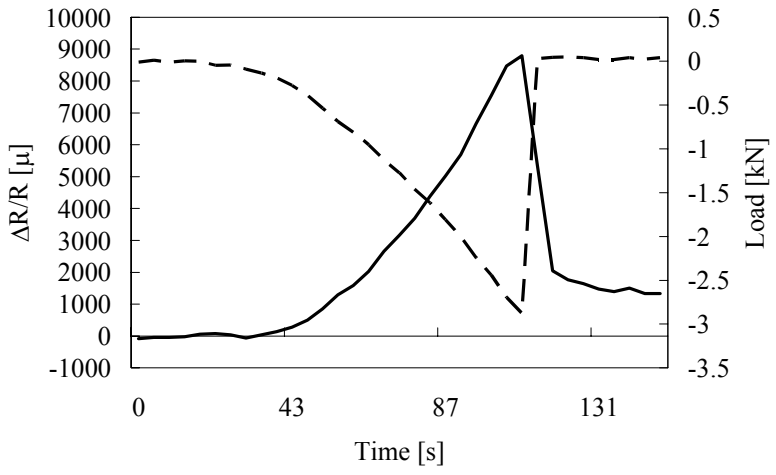

Fig.5 Load-displacement and electrical resistance change-displacement curves.

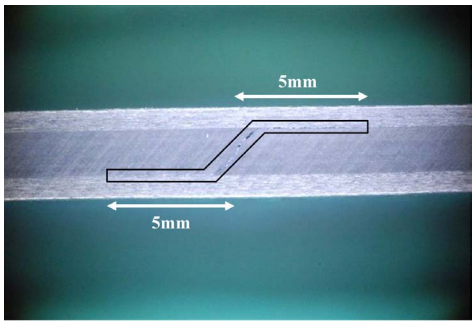

Fig.6 Specimen side surface of delamination cracking.

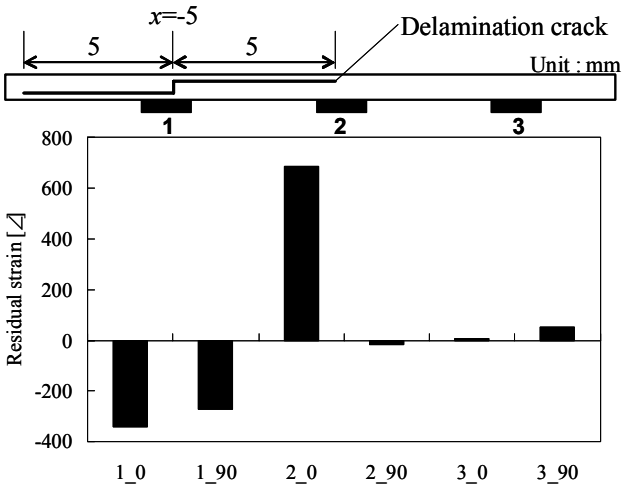

Fig.7 Measured residual strain relief after delamination cracking.

Table 1. Measured electric conductivity.

Measure direction	Stacking sequence	Conductivity [S/m]	σ_{90}/σ_0	σ_t/σ_0
σ_0	$[0]_8$	4100	-	-
σ_{90}	$[90]_8$	3.3	8.1×10^{-4}	-
σ_t	$[0/90]_{2s}$	1.1	-	2.6×10^{-4}
	$[0_2/90_2]_s$	1.0	-	2.5×10^{-4}
	$[0/90/\pm45]_{2s}$	0.8	-	2.0×10^{-4}
	$[0/90]_{4s}$	1.8	-	4.5×10^{-4}

Table 2 Material properties used for FEM analyses

Material	PYROFIL #380 (Carbon/Epoxy)		
Direction	x (xy)	y (yz)	z (zx)
E [Gpa]	141	10	10
G [GPa]	5.0	0.15	5.0
ν	0.3	0.4	0.3
α [10^{-6}/K]	0.9	30	30
σ [S/m]	4100	3.3	3.3

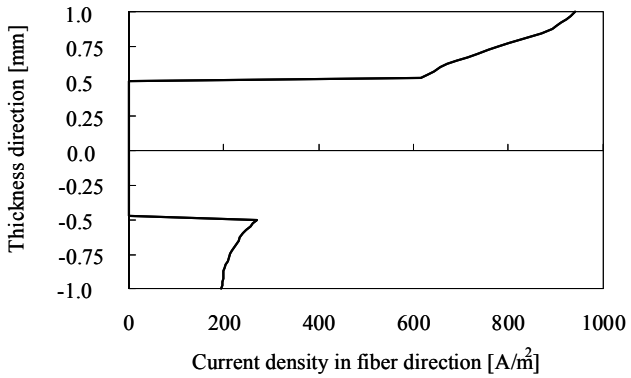

Fig.8 Electric current density (x-direction) distribution by FEM

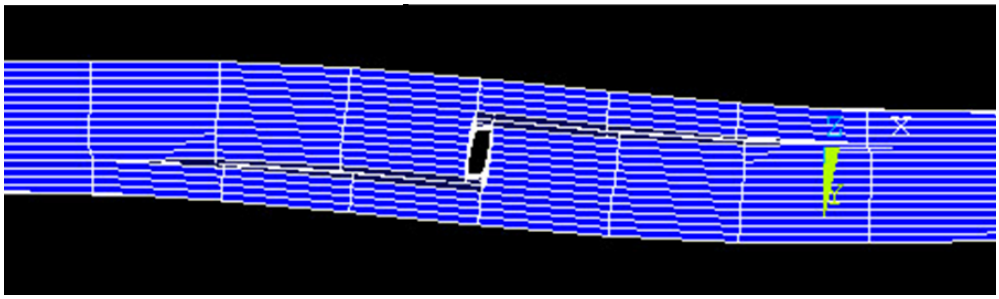

Fig.9 Magnified deformation of FEM result after delamination cracking with consideration of residual strain relief.

Table 1 shows the results of the electric conductivity measurements. Since the conductivities in the thickness direction of the various stacking sequences did not scatter to a significant extent, the results show that the conductivity was not affected by differences of the stacking sequence. Table 2 shows the material property values used for the FEM analyses.

Figure 8 shows the FEM results of electric current density of the specimen without a delamination crack. The ordinate is the depth from the top surface where the electrodes are located. The abscissa is the electric current density. Since the top and bottom plies were 0°-plies and the middle was a 90°-ply, electric current density is almost non-existent in the middle ply. The figure shows that almost 70 % of the electric current flows in the top 0°-ply. This implies that the calculation of the effect of the piezoresistance may count only the electric current of the top 0°-ply.

To obtain the residual strain relief, two FEM analyses were performed. The first calculation used the FEM model without a delamination crack, and the second used the FEM model with a delamination crack. Using both specimens, thermal deformations were calculated during cooling from the maximum curing temperature to room temperature. The strain results of the first model were subtracted from the results of the second model. For the FEM calculation of the second model the observed actual reversed–type delamination crack configuration was adopted.

Figure 9 shows the results of deformation after delamination cracking, with residual strain relief magnified to visually confirm the deformation. This implies that the delamination crack is fully open after the delamination cracking when the residual strain relief is considered, and the deformation is not uniform in the top ply. This non-uniform delamination is caused by the reversed Z-type configuration of the delamination crack. Since the tension strain has the reverse effect of piezoresistance compared to the compression strain, the effect of the piezoresistance of the top 0°-ply requires integration of the relieved strain in the top surface to evaluate the effect of the piezoresistance after delamination creation.

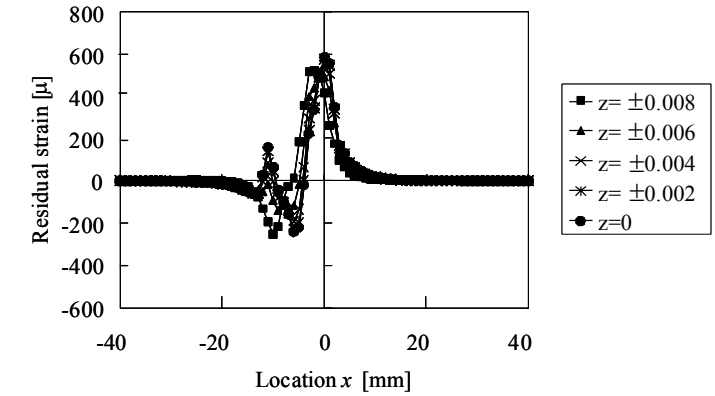

(a) Residual strain relief of x-direction strain

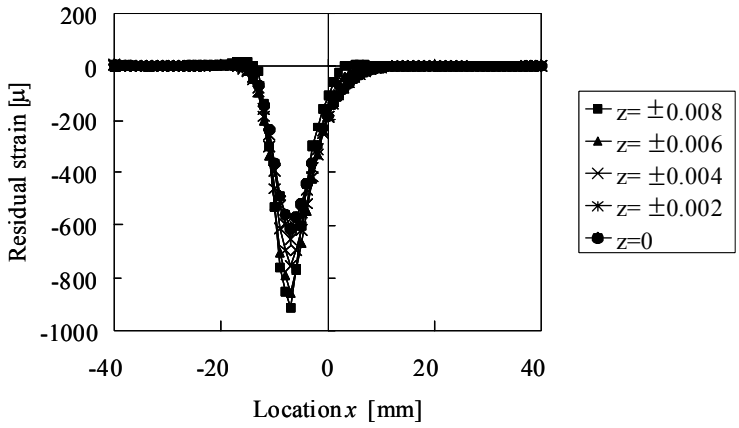

(b) Residual strain relief of y-direction strain.

Fig.10 Residual strain relief from FEM results.

Figure 10 (a) and (b) shows the results of the residual strain relieved by delamination creation, calculated by the FEM analyses. The ordinate is the calculated residual strain at the top 0°-ply surface at various width locations (z-location), and the abscissa is the x-axis coordinate. As shown in Fig.10, the residual strain distributions showed complicated configurations. For the calculations of the effect of piezoresistance, the strain distributions were averaged between the electrodes (from x=-15 mm to x=15 mm). The approximated averaged value of the residual strain in the region between the electrodes was 100 μ in the fiber direction and -200 μ in the transverse direction. Since the residual strain is the maximum at the surface, the averaged residual strain at the surface means maximum estimation of the effect of piezoresistance.

To confirm the FEM results they were compared with the experimental results. Figure 11 (a) and (b) shows the results of the comparisons. The broken curves show the FEM results and the square symbols show the experimentally measured residual strains: the FEM results agreed well with the experimental data. These results reveal that the FEM analyses were acceptable although there is small error, and the estimation of the averaged residual strain was approximately the maximum estimation of the effect of the piezoresistance. Substituting the estimated averaged residual strain in Eq. (1) yields the electrical resistance change caused by the piezoresistance. The substitution results were as follows.

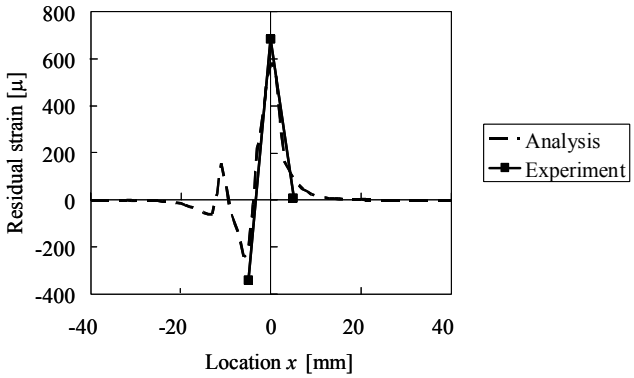

(a) x-direction strain

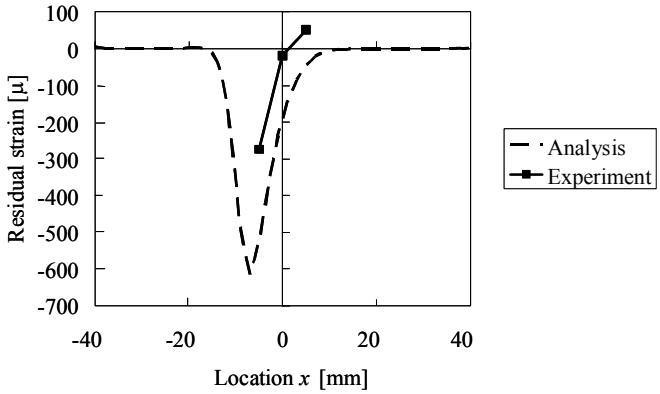

(b) y-direction strain

Fig.11 Comparison of residual strain relief of FEM results with experimental results

$$\begin{Bmatrix} \left(\frac{\Delta R}{R}\right)_L \\ \left(\frac{\Delta R}{R}\right)_T \end{Bmatrix} = \begin{bmatrix} 2.49 & 0.43 \\ -0.42 & 2.38 \end{bmatrix} \begin{Bmatrix} 100\mu \\ -200\mu \end{Bmatrix} = \begin{Bmatrix} 163\mu \\ -518\mu \end{Bmatrix} \tag{2}$$

The FEM result of the shut-off of current path indicates that the electrical resistance increase was 1525 μ. The experimental result shows the electrical resistance increase was 1330 μ. The sum of the FEM analyses effects was 163 μ + 1525 μ=1690 μ. The error compared to the experimental result is only 27%, although the present study adopts rough estimation of the effect of the residual strain relief. Since the effect of the piezoresistance was the maximum estimation, this error means the result agrees well with the experimental result, and indicates that the electrical resistance change of the thin CFRP laminate was mainly caused by the effect of shut-off of current path, and the effect of the piezoresistance was negligible compared to the shut-off effect. The detail FEM analysis with considering delamination surface contact may improve the error. This result supports reducing the number of experiments with FEM analyses, as discussed previously [23]. The electrical resistance change can be estimated only by the shut-off effect with the FEM analyses for the thin CFRP laminates, and the results show excellent agreement with the experimental results. As noted above, electrical resistance decreases after delamination cracking of a thick CFRP laminate. The difference compared to the thin CFRP laminate may require another mechanism. This is a topic for our future work.

5. Conclusion

This paper examines the mechanism of electrical resistance change after delamination cracking of a thin CFRP laminate. The effects of shut-off of the current path and piezoresistance caused by residual strain relief are investigated analytically and experimentally. FEM analyses of residual strain relief show good agreement with experimental results obtained using strain gages. Multi-axis piezoresistance is applied to estimate the magnitude of the piezoresistance effect. Comparison of the experimental results with the FEM analyses show that the electrical resistance increase after delamination cracking of the thin CFRP laminate is caused by the effect of shut-off of the current path. The piezoresistance has only a small effect for the thin CFRP laminate.

References

(1) Schulte, K. and Baron, Ch. Load and failure analyses of CFRP laminates by means of electrical resistivity measurement, *Composites Science and Technology*, Vol.36, No.1, (1989) pp.63-76.

(2) Muto, N. Yanagida, H., Nakatsuji, T., Sugita M., and Ohtsuka Y., Preventing fatal fractures in carbon-fiber glass-fiber-reinforced plastic composites by monitoring change in electrical resistance, *J. Am. Ceram. Soc*., Vol.76, No.4, (1993), pp.875-879.

(3) Wang X. and Chung D.D.L., Sensing delamination in a carbon fiber polymer-matrix composite during fatigue by electrical resistance measurement, *Polymer Composites*, Vol.18, No.6 ,(1997), pp.692-700.

(4) Irving P.E. and Thiagarajan C., Fatigue damage characterization in carbon fibre composite materials using an electrical potential technique, *Smart materials and structures*, Vol.7, No.4, (1998), pp.456-466.

(5) Abry J.C., Bochard S., Chateauminois A., Salvia M. and Giraud G., In situ detection of damage in CFRP laminates by electric resistance measurements, *Composites Science and Technology*, Vol.59, No.6, (1999), pp.929-935.

(6) Seo D.C. and Lee J.J., Damage detection of CFRP laminates using electrical resistance measurement and neural network, *Composite structures*, Vol.47,No.1-4, (1999), pp.525-530.

(7) Wang S. and Chung D.D.L., Piezoresistivity in continuous carbon fiber polymer-matrix composite, Polymer Composites, Vol. 21, No.1, (2000), pp.13-19.

(8) Schueler R., Joshi S.V. and Schulte K., Damage detection in CFRP by electrical conductivity mapping , *Composites Science and Technology*, Vol.61, No.6, (2001),pp.921-930.

(9) Park J. B., Okabe T., Takeda N. and Curtin W. A., Electromechanical modeling of unidirectional CFRP composites under tensile loading condition, *Composites Part A*, Vol.33, No.2, (2002), pp.267-275.

(10) Ogi K.and Takao Y., Characterization of piezoresistance behavior in a CFRP unidirectional laminate, *Composites Science and Technology*, Vol.65, No.2, (2005),pp.231-239.

(11) Todoroki A., and Yoshida J., Electrical resistance change of unidirectional CFRP due to applied load , *JSME International J., Series A*, Vol.47, No.3,(2004)pp. 357-364.

(12) Todoroki A., Samejima Y., Hirano Y., and Matsuzaki R., Piezoresistivity of Unidirectional Carbon/epoxy Composites for Multiaxial Loading, Composites Science and Technology,69, 11, (2009), pp.1841-1846.

(13) Todoroki A., Omagari K., Shimamura Y., and Kobayashi H., Matrix crack detection of CFRP using electrical resistance change with integrated surface probes, *Composites Science and Technology*, Vol.66, No.11-12, (2006), pp 1539-1545.

(14) Todoroki A., and Omagari K., Detection of matrix crack density of CFRP using electrical potential change method with multiple probes, *Journal of Solid Mechanics and Materials Engineering, JSME*, Vol.2, No.6, (2008), pp.718-729.

(15) Todoroki A., Matsuura K., and Kobayashi H., Application of Electric Potential Method to Smart Composite Structures for Detecting Delamination, *JSME International J., Series A*, Vol.38, No.4, (1995),pp.524-530.

(16) Todoroki A., Effect of number of electrodes and diagnostic tool for delamination monitoring of graphite/epoxy laminates using electric resistance change, *Composites Science and Technology*, Vol.61,No.13,(2001),pp.1871-1880.

(17) Todoroki A., and Tanaka Y., Delamination identification of cross-ply graphite/epoxy composite beams using electric resistance change method, *Composites Science and Technology,* Vol. 62, No.5, (2002), pp.629-639.

(18) Todoroki A., Tanaka Y., and Shimamura Y., Delamination monitoring of graphite/epoxy laminated composite plate of electric resistance change method, *Composites Science and Technology*, Vol. 62, No.9,(2002), pp.1151-1160.

(19) Todoroki A., Tanaka M., and Shimamura Y., Measurement of orthotropic electric conductance of CFRP laminates and analysis of the effect on delamination monitoring with electric resistance change method, *Composites Science and Technology*, Vol.62, No.5, (2002), pp.619-628.

(20) Todoroki A., Tanaka M. and Shimamura Y., High performance estimations of delamination of graphite/epoxy laminates with electric resistance change method, *Composites Science and Technology*, Vol.63, No.13, (2003), pp.1911-1920.

(21) Ueda M., Todoroki A., Shimamura Y. and Kobayashi H., Monitoring Delamination of Laminated CFRP using the Electric Potential Change Method (Two-stage monitoring for robust estimation), *Advanced Composite Materials*, Vol. 14, No.1, (2005), pp.83-98.

(22) Todoroki A., Ueda M. and Shimamura Y., Damage Monitoring of Thick CFRP Beam Using Electrical Impedance Changes, *Key Engineering Materials*, Vol. 353-358, (2007), pp.1298-1301.

(23) Todoroki A. and Ueda M., Low Cost Delamination Monitoring of CFRP Beams Using Electrical Resistance Changes With Neural Networks, *Smart Materials and Structures*, Vol. 15, No.4,(2006), pp.N75-N85.